ADVANCED FUNCTIONAL MATERIALS
www.afm-journal.de

Materials Views
www.MaterialsViews.com

Epindolidiones—Versatile and Stable Hydrogen-Bonded Pigments for Organic Field-Effect Transistors and Light-Emitting Diodes

Eric Daniel Głowacki, Giuseppe Romanazzi, Cigdem Yumusak, Halime Coskun, Uwe Monkowius, Gundula Voss, Max Burian, Rainer T. Lechner, Nicola Demitri, Günther J. Redhammer, Nevsal Sünger, Gian Paolo Suranna and Serdar Sariciftci*

Hydrogen-bonded pigments are remarkably stable high-crystal lattice energy organic solids. Here a lesser-known family of compounds, the epindolidiones, which demonstrates electronic transport with extraordinary stability, even in highly demanding aqueous environments, is reported. Hole mobilities in the range 0.05–1 $cm^2 V^{-1} s^{-1}$ can be achieved, with lower electron mobilities of up to 0.1 $cm^2 V^{-1} s^{-1}$. To help understand charge transport in epindolidiones, X-ray diffraction is used to solve the crystal structure of 2,8-difluoroepindolidione and 2,8-dichloroepindolidione. Both derivatives crystallize with a linear-chain H-bonding lattice featuring two-dimensional π–π stacking. Powder diffraction indicates that the unsubstituted epindolidione has very similar crystallinity. All types of epindolidiones measured here display strong low-energy optical emission originating from excimeric states, which coexists with higher-energy fluorescence. This can be exploited in light-emitting diodes, which show the same hybrid singlet and low-energy excimer electroluminescence. Low-voltage FETs are fabricated with epindolidione, which operate reliably under repeated cyclic tests in different ionic solutions within the pH range 3–10 without degradation. Finally, in order to overcome the insolubility of epindolidiones in organic solvents, a chemical procedure is devised to allow solution-processing via the introduction of suitable thermolabile solubilizing groups. This work shows the versatile potential of epindolidione pigments for electronics applications.

1. Introduction

Hydrogen-bonded organic pigments are a class of materials familiar from applications in the colorant industry, where they find widespread use as materials for robust outdoor paints, cosmetics, and printing inks.[1,2] Indigo, a natural product, is the oldest and still most widely produced organic dye and pigment (**Figure 1**).[3] The intermolecular –NH···O = hydrogen bonding that characterizes indigo is exploited in most of the synthetic hydrogen-bonded pigments as well. This class of materials has proven to be nontoxic and safe for humans, and is considered safer than even several classes of food dyes.[4] Hydrogen-bonding as a supramolecular engineering tool is useful to control self-assembly and highly relevant to aqueous and biochemical systems.[5,6] Recently, we have found that indigo,[7] and some of its derivatives[8,9] demonstrate ambipolar transport in organic field-effect transistors (OFETs), with mobility ranging from 0.01–0.4 $cm^2 V^{-1} s^{-1}$. We

Dr. E. D. Głowacki, Dr. C. Yumusak, H. Coskun, Dr. G. Voss, Prof. S. Sariciftci
Linz Institute for Organic Solar Cells (LIOS)
Johannes Kepler University
A-4040, Linz, Austria
E-mail: eric_daniel.glowacki@jku.at

Dr. G. Romanazzi, Prof. G. P. Suranna
Dipartimento di Ingegneria Civile
Ambientale, del Territorio
Edile e di Chimica (DICATECh)
Politecnico di Bari, Via Orabona 4
70125, Bari, Italy

Dr. C. Yumusak
Department of Physics, Faculty of Arts and Sciences
Yildiz Technical University, Davutpasa Campus
Esenler 34210, Istanbul, Turkey

DOI: 10.1002/adfm.201402539

Prof. U. Monkowius
Institute of Inorganic Chemistry
Johannes Kepler University
A-4040, Linz, Austria

M. Burian, Prof. R. T. Lechner
Institute of Physics, Montanuniversitaet Leoben
Franz-Josef-Strasse, 18, 8700, Leoben, Austria

Dr. N. Demitri
Elettra – Sincrotrone Trieste, S. S. 14 Km 163.5 in Area Science Park
34149, Basovizza, Trieste, Italy

Prof. G. J. Redhammer
Materialwissenschaften und Physik
Abteilung für Mineralogie, Paris-Lodron Universität Salzburg
Hellabrunner Str. 34 5020, Salzburg, Austria

N. Sünger
Solar Energy Institute
Ege University
Izmir, Turkey

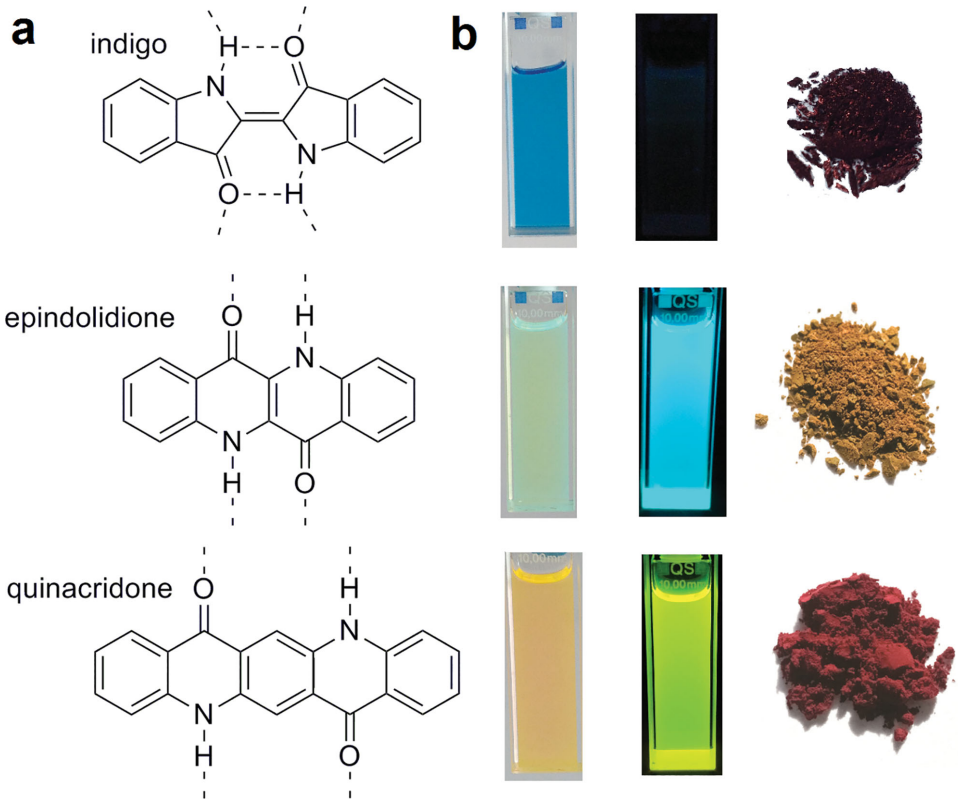

Figure 1. a) Molecular structures of indigo, its isomer epindolidione, and quinacridone. Dashed lines indicate hydrogen-bonding. b) 0.1 mM solutions of each material in DMSO, with photoluminescence excited at 365 nm. While epindolidione and quinacridone are highly emissive, indigo has very low luminescence quantum yield. The powders of the three pigments are shown on the right, where the bathochromically shifted absorption and tinctorial strength are visible.

then reported on quinacridone, a common industrial colorant perhaps best known as constituting the magenta printer pigment, as an ambipolar semiconductor with mobility in the 0.01–0.1 $cm^2\ V^{-1}\ s^{-1}$ range (Figure 1).[10] Quinacridone also demonstrated the formation of low-energy luminescent species, attributed to charge transfer excitons, which led to a low effective exciton binding energy and promising photovoltaic behavior.[11] Alongside quinacridone, we evaluated its 4-ring analog epindolidione (Figure 1). Epindolidione demonstrated promising behavior in OFETs, providing hole mobility as high as 1.5 $cm^2\ V^{-1}\ s^{-1}$ with excellent stability in air.[10] Indigo, epindolidione, and quinacridone are all examples of hydrogen-bonded pigments where interplay between intermolecular H-bonds and π–π stacking interactions lead to strong intermolecular interactions and high crystal lattice energy solids.[1,2,12] A substantial bathochromic shift in absorption accompanied by increased oscillator strength occurs from dilute solutions to the solid state (Figure 1b). Intramolecular H-bonding in indigo results in ultrafast proton transfer in the excited state, quenching luminescence.[13] Quinacridone and epindolidione, in contrast, are highly luminescent in solution. Epindolidione is a structural isomer of indigo, however photophysically, it is very different—it is highly luminescent, even in the solid state, and is yellow/orange, instead of blue. Additionally, as we report here, it crystallizes with a very different structure than indigo. In this work, we follow up on the epindolidione class of compounds, detailing synthetic preparation and characterization of epindolidiones, their crystalline structure, optical and electrochemical properties, and results from OFETs and electroluminescent devices. Finally, we revisit the issue of epindolidione OFET stability, showing also that such devices can operate with excellent stability without any passivation even in aqueous environments within a pH range from 3–10.

2. Results and Discussion

2.1. Synthesis and Characterization of Epindolidiones

The synthetic approach followed to obtain the epindolidiones: *dibenzo[b,g][1,5]naphthyridine-6,12(5H,11H)-dione* (Epi), *2,8-difluorodibenzo[b,g][1,5]naphthyridine-6,12(5H,11H)-dione* (2F-Epi), *2,8-dichlorodibenzo[b,g][1,5]naphthyridine-6,12(5H,11H)-dione* (2Cl-Epi) is detailed in **Scheme 1** and follows the procedure reported by Jaffe and Matrick,[14] although the suggestions by Kemp et al.[15] concerning the preparation of intermediates 1–3 have also been taken into account. Dimethyl dihydroxyfumarate (1) reacts rapidly with aniline, or *p*-fluoroaniline or *p*-chloroaniline, under hydrochloric acid catalysis to give precipitation of dimethyl bis(arylamino)maleates 2a-c in high yields. The *Z* geometry of 2a-c was confirmed by ^1H NMR spectra as well as by the presence of a very strong FT-IR absorption at 1570 cm^{-1} ascribable to the olefinic stretching of maleate. In boiling Dowtherm A and under high dilution, maleates 2a-c

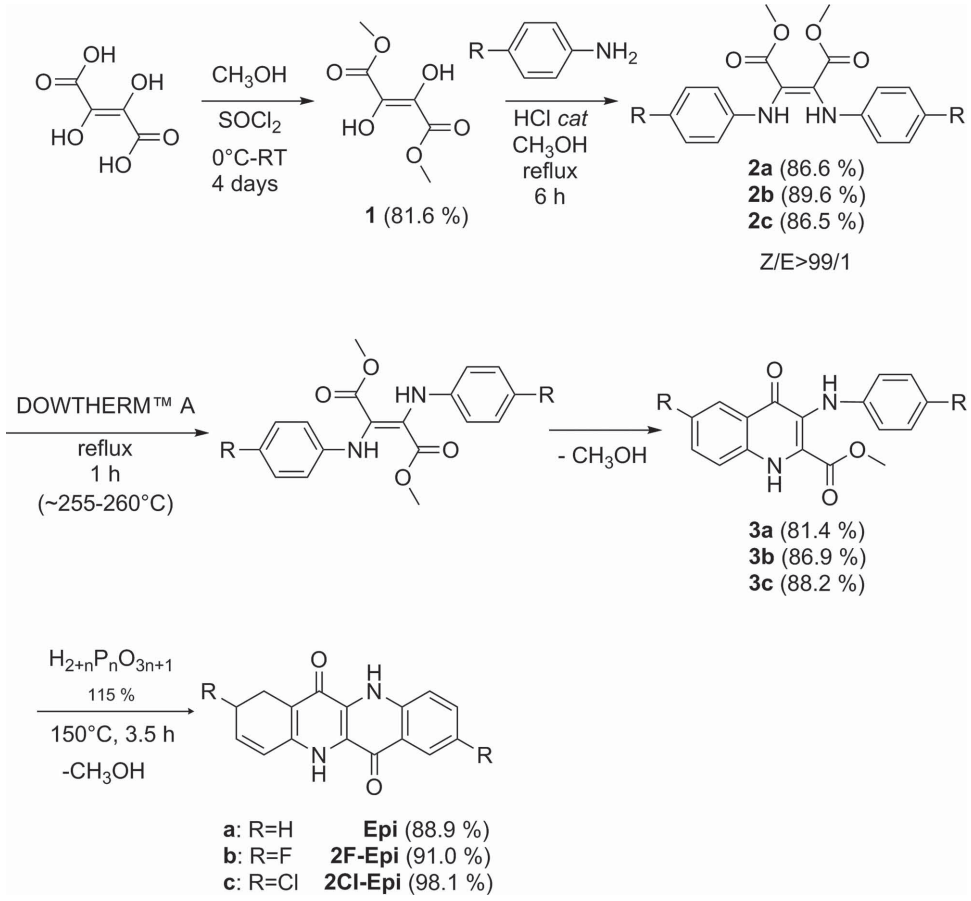

Scheme 1. Synthetic procedure for preparing epindolidiones from *para*-substituted anilines.

isomerize into dimethyl bis(arylamino)fumarates, which then undergo the expected Conrad-Limpach cyclization to give the corresponding carbomethoxyquinolones 3a-c in high yields. Eventually, ring closure of 3a-c to give Epi, 2F-Epi, and 2Cl-Epi respectively was carried out at 150 °C in polyphosphoric acid (PPA) under high dilution conditions. After hydrolysis of the PPA solution, epindolidiones Epi, 2F-Epi, 2Cl-Epi precipitated as greenish yellow to yellow powders; overall yields with respect to the initial amount of dihydroxyfumaric acid were 51.1%, 57.8%, and 61.1% respectively. The target molecules Epi, 2F-Epi, 2Cl-Epi are very sparingly soluble in common organic solvents, however, their structures could be confirmed by solution ^{1}H NMR in deuterated dimethyl sulfoxide (DMSO-d_6) or deuterosulfuric acid (D_2SO_4). Their purity was assessed by CHN elemental analysis. This synthetic procedure can in principle be applied to a wide range of substituted anilines, many of which are well-known commercially available materials. Thus many epindolidione derivatives can be prepared from cheap aniline building blocks.

2.2. Solubilization of Epindolidione by *t*-butoxycarbonylation (tBOC Protection)

The very poor solubility in common organic solvents of Epi limits its thin-film processability to vacuum-evaporation. It also precludes further synthetic chemical derivatization. Thus, the latent pigment approach was pursued in order to obtain a soluble material suitable for solution-processing or further chemical manipulation. Applied to epindolidione, this approach consists of the reaction of the N–H group with di-*tert*-butyl dicarbonate $(tBOC)_2O$, a well-known protecting group for amine functions. As a result, the H-bond network is transiently disrupted, leading to a solubility improvement of orders of magnitude and thereby, allowing solution processing. The tBOC groups are subsequently removed by simple heating (or by acid treatment) with the release of gaseous CO_2 and isobutene. This procedure was introduced for insoluble industrial pigments like diketopyrrolopyrroles and quinacridones by researchers at the Ciba-Geigy company.[16,17]

Contrary to other H-bonded pigments, which can readily be functionalized with tBOC according to several simple procedures,[16–18] the t-butoxycarbonylation of Epi proved to be quite a demanding task. After several attempts, we were able to find the best protocol (**Scheme 2**) in terms of yields and reaction time. A stoichiometric amount of 4-dimethylaminopyridine (DMAP) and a large excess of $(tBOC)_2O$ were necessary to obtain, after flash chromatography, di-tBOC Epi, and mono-tBOC Epi. The persistence of a significant amount of mono-tBOC Epi in the reaction mixture is likely caused by the stability of the *enol* tautomeric form of this compound. ^{1}H NMR of mono-tBOC Epi in chloroform confirms that the hydroxyquinoline tautomer is

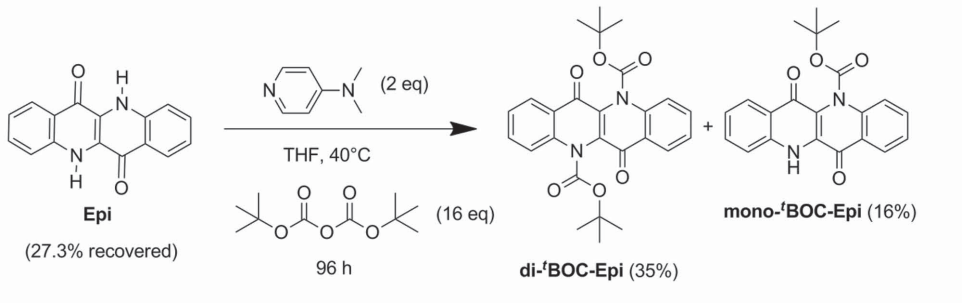

Scheme 2. Protection reaction to obtain tBOC-functionalized epindolidione.

dominant at equilibrium in solution, explaining why the reaction with a second tBOC group is impeded.

The tBOC derivatives proved to be, as expected, highly soluble: the solubility of di-tBOC Epi reaches concentrations up to ≈25 mg mL^{-1} in chloroform. Solution processing of films using di-tBOC Epi is described in detail in Section 2.8.

2.3. Crystal Structure

An important step in understanding the charge transport in H-bonded epindolidione pigments is to evaluate the solid state structure of such materials. Diffraction-quality single crystals of hydrogen-bonded pigments can typically be grown using physical vapor transport recrystallization. Establishing the crystal structure of the closely related quinacridone family of pigments presented a challenge to crystallographers for many years, as growing defect-free crystals of suitable size required considerable trial-and-error optimization. Details concerning this long-term effort were the subject of three review articles on quinacridone crystallography.[19–21] We encountered similar problems, and were unable despite many attempts to grow suitable crystals of Epi using vapor or solution-based methods. These crystals were either very small, in the <10 μm range, or had multiple twinning defects. However, successful crystal growth was achieved with 2F-Epi and 2Cl-Epi. The materials were first purified twice via temperature-gradient sublimation and then loaded into an alumina crucible and heated to 330–350 °C in a borosilicate glass tube under a 2 L min^{-1} flow of dry N_2 gas. Over the course of 3–5 days, large single crystals grew in the downstream 110–130 °C zone of the glass tube. 2Cl-Epi crystals could be measured using Mo K_α radiation on a standard Bruker diffractometer. The smaller 2F-Epi crystals were measured using 0.7 Å synchrotron radiation. Both materials crystallize in the same fashion: projections of the crystal structure of 2F-Epi are shown in **Figure 2**. The powder diffraction data for the two halogenated materials is compared with the parent molecule epindolidione in Figure S1, Supporting Information, and based on the close similarity of the diffraction patterns it is likely the Epi crystallizes in the same fashion as its measured derivatives. The two halogenated derivatives crystallize with a linear-chain H-bonding lattice featuring two-dimensional π–π stacking, very similar to the quinacridone α_I phase.[21] Molecules are H-bonded to two neighbors, forming infinite linear chains which are parallel to each other. These linear chains are π–π stacked on top of each other in a brick-wall pattern. The NH···O= H-bond length is very short: 2F-Epi, (2Cl-Epi, in parenthesis); 2.05 (2.06) Å, close to that found in the quinacridone α_I phase (2.01 Å). Indigos, for comparison, have H-bond lengths of 2.1–2.8 Å. Intermolecular distances for stacking interactions are 3.9 Å (3.69 Å) along a, and 6.2 Å (5.97 Å) along b. As in the case of other H-bonded pigment semiconductors, it is concluded that charge transport primarily occurs perpendicular to the H-bonding plane, along the two π-stacking directions. It cannot be excluded that, as was recently proposed for close H-bond interactions in diketopyrrolopyrrole compounds,[22] that a significant probability of charge transport along the H-bonded chains also exists. The short H-bond lengths and close stacking interactions are together accountable for the high crystal lattice energy of epindolidione pigments, as observed by thermogravimetric (TGA) analysis (**Figure 3**). All three epindolidione pigments were found to sublime cleanly, leaving no charred residue, at sublimation temperatures >405 °C. This high sublimation point is indicative of strong intermolecular interactions and high crystal lattice energy. As a reference example, tetracene has an analogous structure and similar molecular weight, but sublimes at 280 °C under the same experimental conditions.[10] We were not successful to grow diffraction-quality crystals of the tBOC-epindolidiones. Deprotection of these compounds occurs at 190 °C, followed by sublimation at the same temperature as the measured unsubstituted epindolidione (Figure 3). The % weight loss corresponds to tBOC groups leaving, based on previous reports of tBOC decomposition, we assume that decarboxylation occurs and these groups decompose into CO_2 and isobutene.[23] TGA confirms the successful regeneration of H-bonded epindolidione following thermal deprotection.

2.4. Optical Properties

Epindolidiones described in the patent literature are pigments with yellow or orange color. All three derivatives described here are yellow powders. The solubility of the epindolidiones is very poor in organic solvents, but they can be dissolved at concentrations $<200 \times 10^{-6}$ M in polar aprotic solvents such as dimethyl sulfoxide (DMSO) and dimethylformamide (DMF) after heating and sonication. **Figure 4**a shows the extinction coefficients of Epi, 2F-Epi, 2Cl-Epi dissolved in DMSO. A typical vibronic progression is clear for all compounds. Epindolidiones are isomers of indigo, and contain a similar cross-conjugated π-system.

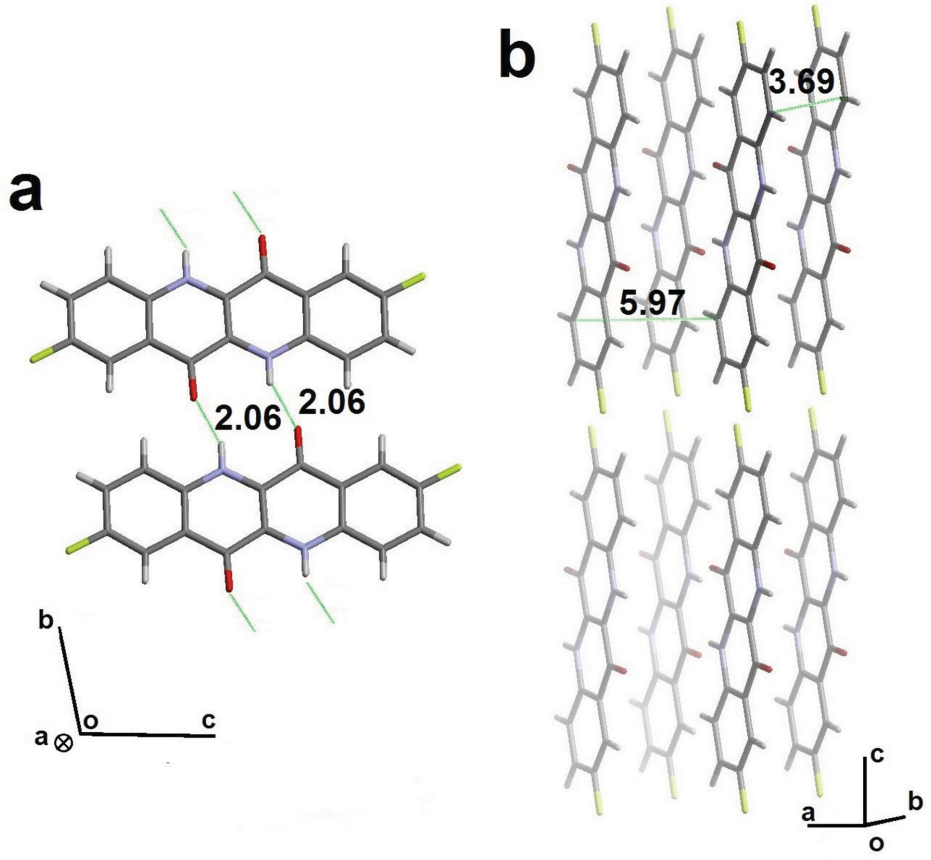

Figure 2. Crystal structure of 2F-Epi obtained from single-crystal X-ray diffraction using synchrotron radiation with a wavelength of 0.7 Å. a) View down the a axis showing the propagation of linear H-bonded chains of molecules. b) View down the b-axis with π–π stacking interactions (with intermolecular distances in units of Å shown in green). The measured crystal structure of 2Cl-Epi is qualitatively identical to this one.

For indigo, the cross-conjugated arrangement of electron-rich NH groups with the electron-withdrawing carbonyl functions produces the so-called H-chromophore, which supports a low-energy charge-transfer type absorption.[9,24] Our observations on the three epindolidione derivatives appear to support the hypothesis that they are indeed H-chromophore systems as well. If epindolidiones are treated as an H-chromophore system like the cross-conjugated indigos, the presence of a π-electron donor *para* to the nitrogen (donor component in the H-chromophore) should shift absorption bathochromically by virtue of increasing the donor ability of the NH groups. This is consistent with the observation that the halogenated compounds have a ≈10 nm bathochromic shift in absorption onset compared to the unsubstituted Epi. Photoluminescence and excitation spectra for Epi, 2F-Epi, and 2Cl-Epi are shown in panels b, c, and d, respectively, of Figure 4. While the halogenated derivatives show a typical Franck–Condon mirror-image luminescence spectrum, for unsubstituted Epi the highest energy luminescence peak is weak compared with the next lower-energy PL peak. The origin of this effect is unclear. The PL yields of epindolidiones in solution are high,[25] much higher than in the case of indigos. Indigos undergo a photoinduced intramolecular proton transfer, leading to a tautomerization reaction followed by relaxation, leading to overall efficient radiationless internal conversion and very weak photoluminescence ($\phi_f = 1 \times 10^{-3}$).[9,13] This tautomerization mechanism is blocked in the case of epindolidione by their fused-ring structure. Therefore, epindolidiones can be regarded as H-chromophoric molecules without a proton-mediated relaxation pathway and thus

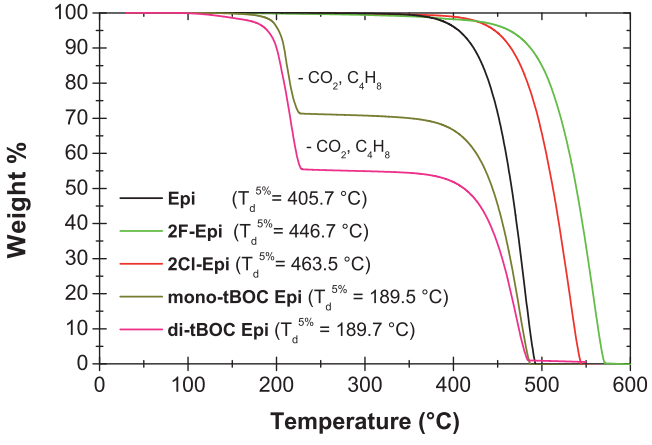

Figure 3. TGA scans for the three epindolidiones and the mono- and di-tBOC epindolidione. In the latter case, the loss of the tBOC groups is clearly visible.

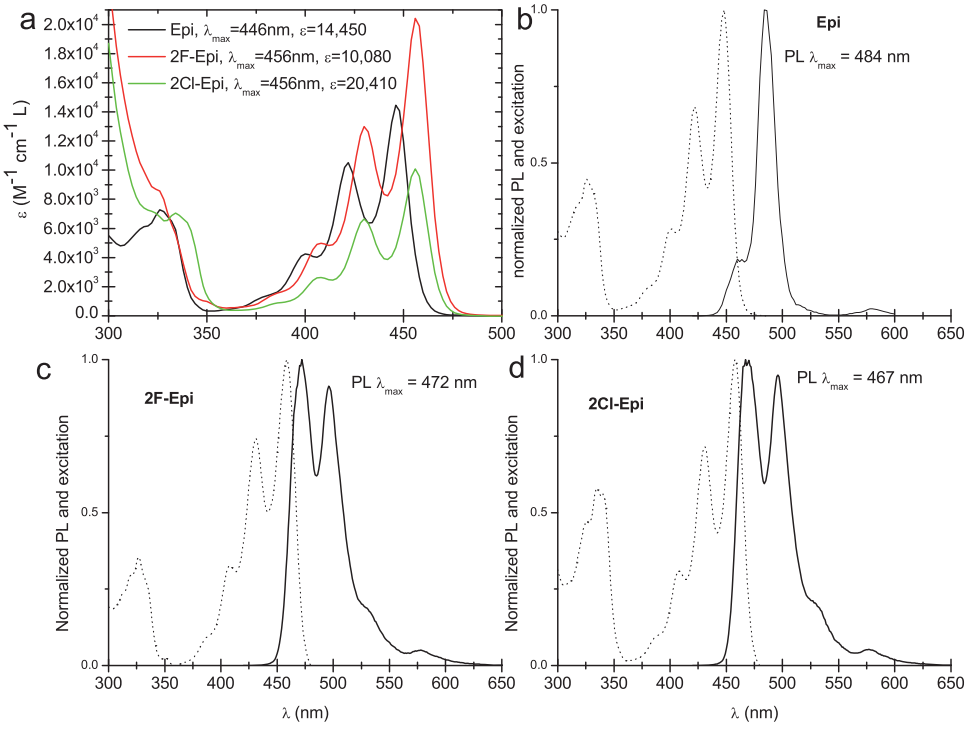

Figure 4. a) UV–vis absorption and photoluminescence of 0.1 mM solutions of the three epindolidiones in DMSO. b) PL and excitation spectra for 0.01mM Epi in DMSO. c) PL and excitation spectra for 0.1 mM 2F-Epi in DMSO. c) PL and excitation spectra for 0.1 mM 2Cl-Epi.

high luminescence. In the case of Epi, we found a reproducible aggregation effect, shown in Figure S2, Supporting Information. Solutions with concentrations greater than 0.1 mM were found to produce aggregates with a distinctive absorption spectrum. We found the exposure of the epindolidione solutions in DMSO to large quantities of HCl, up to 1 M, does not yield any changes in the absorption or emission spectra.

In order to better understand the optical properties of epindolidiones, we carried out density functional theory (DFT) calculations with a 6–311+g(d,p) basis set. The optimized ground state geometries and charge isodensity plots for the HOMO and LUMO orbitals of the three Epi derivatives are shown in **Figure 5**. The HOMO orbitals are concentrated on an extended conjugated segment consisting of the two nitrogen atoms bridged by the central C=C group, while the LUMO orbitals are shifted to the carbonyl functions and C–C units. This is consistent with the H-chromophore model.[24,26] Indeed, the calculated plots for epindolidione are very similar to those of indigo itself.[27] The addition of halogens *para* to the nitrogen groups is thus expected, according to the H-chromophore model, to influence

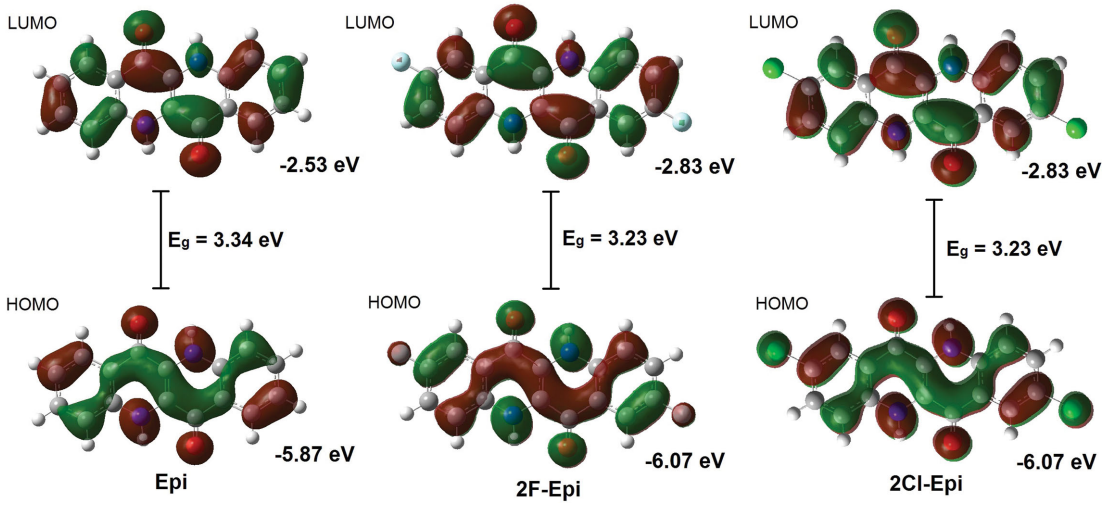

Figure 5. Optimized ground-state geometries and frontier orbital energies of epindolidione and the two halogenated derivatives. The H-chromophore-like distribution of the isodensity plots is very similar to that of indigo.

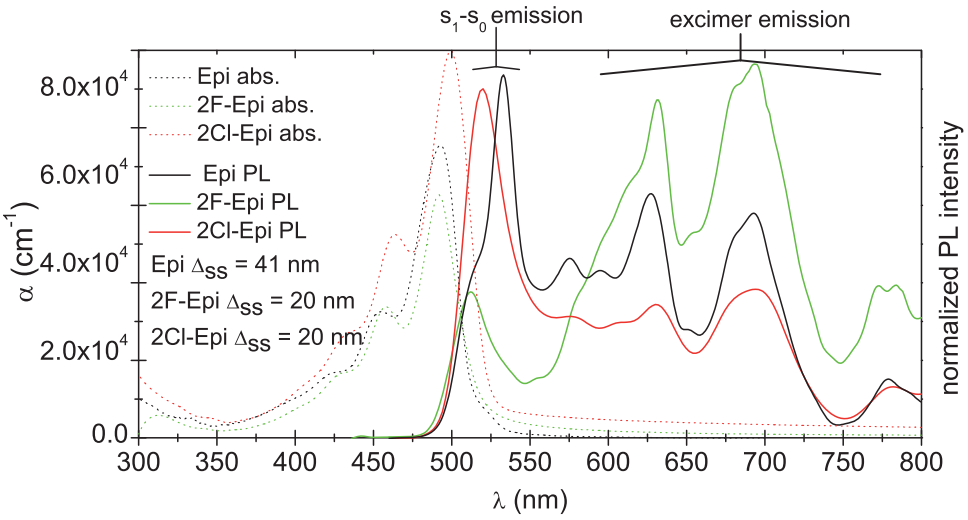

Figure 6. UV–vis absorption and photoluminescence of the three epindolidiones deposited on glass slides.

primarily the HOMO. This is seen in the isodensity plots, where indeed charge density is localized over the halogens in the HOMO but not the LUMO orbitals. According to DFT, both HOMO and LUMO energies are lower than in unsubstituted Epi, leading to smaller band gap, which is observed experimentally as well. Vacuum-evaporated thin films of the three Epi derivatives have absorption onsets bathochromically shifted by about 50 nm relative to solutions (**Figure 6**). This is characteristic of H-bonded pigments, where close lattice packing leads to a large degree of intermolecular electronic interaction.[2] Moreover, the effect of supramolecular mesomerism, where sharing of the proton via H-bonding markedly shifts the electronic properties of such molecules, has also been proposed as an explanation for large bathochromic shifts in H-bonded pigments.[20] The PL of evaporated films features a Stokes-shifted peak in the green, and several peaks far to the red, at roughly 625, 690, and 780 nm for all derivatives. The red-shift for these emissive features is too large to be explained by vibronic replicas, also their oscillator strength is relatively high. Two explanations for these peaks can be put forward: either they originate from extrinsic defect states in the solid-state films, or they are excimeric species. Defect states in such films may arise from impurities, states at grain boundaries between the crystallites, or interfaces between polymorphic forms. It should be stressed that the presence of the low-energy luminescence peaks, as well as their position and relative intensity, was found to be highly reproducible over a wide range of sample preparation conditions. The luminescence features were found to be invariant over evaporation rates of <0.1–6 Å s^{-1}, substrate temperatures of 25–140 °C, post-deposition annealing, as well as solvent annealing procedures which are known to induce rearrangements in H-bonded pigments.[28] Based on the lack of effect of processing conditions, and the high purity of the sublimation-purified material, we propose that extrinsic defect state luminescence is not likely responsible for the low-energy emission, but rather true excimeric species. This hypothesis is further supported by fluorescence microscopy of single crystals (Figure S3, Supporting Information), where both green and red emission is found to originate from the bulk of the crystals. The emission of excimeric species has been extensively studied for the closely related quinacridone family of molecules.[29,30] Both the singlet and excimeric PL features were found to be robust and resistant to degradation under conditions of aging the samples in air, or exposure to water.

2.5. Electrochemical Properties

Cyclic voltammetry was carried out on 80 nm thick films of epindolidiones evaporated on ITO-coated glass functioning as the working electrode. A platinum foil was used as the counter electrode and an Ag/AgCl wire as the pseudo-reference electrode. All three derivatives demonstrated reduction and oxidation behavior (**Figure 7**). Evaluating the reversibility is complicated by the fact that both the reduced and oxidized forms of the epindolidiones are highly soluble in the polar electrolyte solution. Thus, the smaller currents corresponding to the reverse redox processes are caused, in large part, by the substantially diminished quantity of analyte on/near the working electrode. Reduction appears to be quasi-reversible for all three derivatives, while oxidation not so. Epi showed an oxidation onset at 1200 mV (HOMO = –5.6 eV), 2Cl-Epi at 1350 mV (HOMO = –5.7 eV), and 2F-Epi at 1800 mV (HOMO = –5.8 eV). The oxidation potential, not surprisingly, scales with the electronegativity of the halogen substituents. The reduction potential, however, did not display a similar trend. All three derivatives show a reduction peak with an onset of –1500 mV versus Ag/AgCl, corresponding to a LUMO level of approx. –2.9 eV versus vacuum. This is easy to rationalize due to the 2,8 positions of the halogens on the substituted epindolidione molecules according to the H-chromophore model, as discussed in section 2.4. As the halogens are *para* to the NH groups, they have an inductive withdrawing effect on the electron-rich NH part of the molecule, thereby affecting the oxidation potential markedly. However the halogens have no inductive effect on the carbonyl functional groups of the molecule, which are responsible for the electron-accepting properties. From an electrochemical point of view, epindolidiones can be both reduced

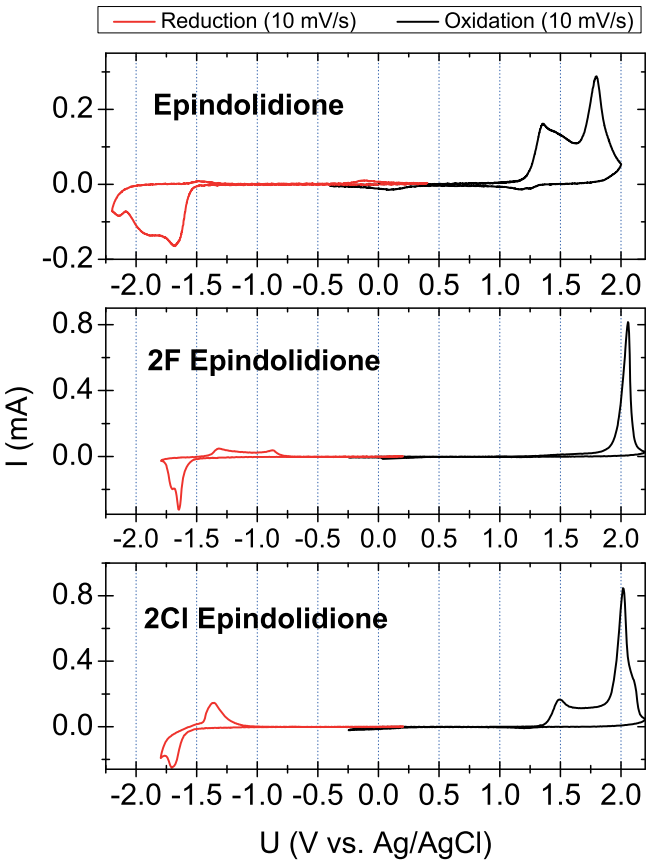

Figure 7. Cyclic voltammetry scans of thin films of different epindolidiones deposited on ITO functioning as the working electrode.

quasi-reversibly, and oxidized, but they are wide band gap materials with relatively high potentials needed to achieve reduction or oxidation.

2.6. Organic Field-Effect Transistors (OFETs)

2.6.1. Measurement of OFETs

OFETs were fabricated with the three Epi derivatives using a 32 nm-thick anodically grown AlO_x passivated with a layer of linear-chain hydrocarbon $C_{44}H_{90}$ (tetratetracontane, or TTC).[9] This composite gate dielectric has a C_{0d} of ≈40 nF cm^{-2}. Mobility was calculated from the saturation regime.[31] The epindolidione layers were evaporated at a rate of ≈0.5 Å s^{-1}, with a total thickness of 80 nm. Top source-drain contacts were evaporated through a shadow mask, giving channel dimensions of W = 2 mm, L = 60 µm. Gold source-drain contacts afforded p-type operation, while aluminum contacts gave n-type behavior. All p-type transistors were measured in ambient air, and were stable for at least 12 months. The n-type transistors, on the other hand, were always measured in an N_2-filled glove box and air-stable mobility was never found. This is not surprising considering the prohibitively high LUMO value for all derivatives. The transfer curve of a typical p-type epindolidione device is shown in **Figure 8**a. Average devices gave mobilities of 0.2 cm^2 V^{-1} s^{-1}, though champion devices had mobilities of around ≈1 cm^2 V^{-1} s^{-1}. Smaller channel lengths can be correlated to higher mobilities, as we previously demonstrated for Epi FETs.[10] With aluminum contacts, Epi showed n-type behavior (Figure 8b), albeit with a significantly lower mobility of 2 × 10^{-3} cm^2 V^{-1} s^{-1}. Based on the LUMO level of –2.9 eV calculated from cyclic voltammetry, it is likely that a significant barrier to electron injection exists and thus contact resistance limits n-type operation. In the case of 2F-Epi (Figure 8c) and 2Cl-Epi (Figure 8d), only n-type mobility could be observed. As evidenced from cyclic voltammetry, the 2,8-halogenated Epis are difficult to oxidize, which probably translates to low hole mobility. This combined with the substantial hole injection barrier is probably the reason for no pFET behavior being observed. While the electron mobility of 2Cl-Epi was relatively low, 2 × 10^{-3} cm^2 V^{-1} s^{-1}, 2F-Epi showed an impressive average electron mobility of 0.1 cm^2 V^{-1} s^{-1}. From these results it is clear that by simple derivitization of the epindolidione core, both n- and p-type behavior can be obtained.

FETs with Epi as the active layer were measured in air over 250 days, with no statistical decline in mobility whatsoever. This correlates with our earlier work,[10] where samples fabricated as part of that study still operate at the same level after ≈2 years.

2.6.2. Stability in Aqueous Environment

Motivated by possible applications of stable FETs for bioelectronics applications,[32] we evaluated the stability of Epi FETs in various aqueous environments. To operate under water, high capacitance gate dielectrics must be used to keep operating voltages in the range of 1–2 V. We utilized anodic aluminum oxide prepared with an anodization voltage of 5V, giving an AlO_x layer with a thickness of ≈8 nm. This layer was then modified by application of an n-octadecyl phosphonic acid self-assembled monolayer, giving a C_{0d} of approx. 350 nF cm^{-2}.[33] An 80 nm-thick epindolidione layer was evaporated on top of the phosphonic acid-modified AlO_x dielectric. Devices with top source-drain contacts of gold were used without any passivation layer, thus the Epi/Au surface layer was in direct contact with the water environment. A poly(dimethylsiloxane) rubber block was used to confine the electrolyte over the entire transistor active area, with a volume of 40 µL of fluid over the FET device. We utilized a test sequence to evaluate OFET performance in a pH range from 3–10 and in the presence of a wide range of various ionic species. Transfer characteristics were measured over 60 cycles in each of a series of different aqueous environments sequentially using a scan rate of 150 mV s^{-1} (**Figure 9**): 18 MΩ high-purity water, pH 7 acetate buffer solution, a pH 7.4 phosphate buffer saline, a pH 4 acetate buffer solution, a pH 3 HCl solution, and a pH 10 NaOH solution. Between measurements the devices were rinsed with deionized water. A total of 360 cycles were measured in this test, plus 10 cycles for dry samples before and after the assay. Devices measured in air with a V_{SD} = –0.5 V exhibited a saturation current of around 100 nA at a V_G = –2.5 V and an on/off ratio of ≈10^3. After 360 cycles in the different aqueous environments the same performance was found, as can be seen comparing the black trace in the first panel of Figure 9 and the blue trace in the final

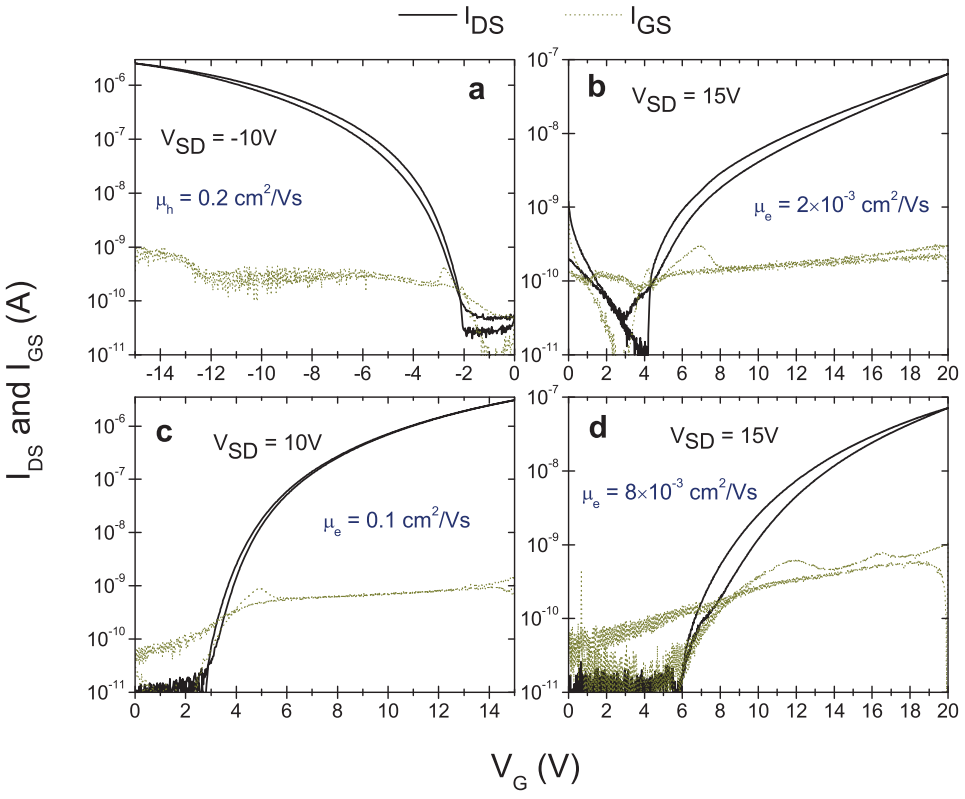

Figure 8. OFET transfer characteristics for a) Epi p-channel with Au source-drain electrodes, b) Epi n-channel with Al source-drain electrodes c) 2F-Epi n-channel with Al electrodes, and d) 2Cl-Epi n-channel with Al source-drain electrodes.

panel. All the "wet" environments featured an off current about 10 times higher than in the dry state, likely due to ionic current between source and drain, or dielectric screening effects. This current does not exceed ≈1 nA and is not dependent on pH, and thus this off-current increase cannot be attributed to doping of the Epi layer. The on current and threshold voltage of the Epi transistors remained constant while cycling under the different electrolyte environments. Previous studies have shown OFETs stable over cycling in pH 7 water,[34] however to our knowledge no study has shown stability in a pH range as wide as that of the present study. This result demonstrating excellent stability in quite demanding aqueous environments suggests that epindolidiones can be highly effective active materials in devices for bioelectronics.

2.7. Organic Light-Emitting Diodes (OLEDs)

Diodes with the structure ITO/PEDOT:PSS/Epi/Al were fabricated in order to evaluate the electroluminescence spectra of the different epindolidione derivatives. *J–V* characteristics are shown in **Figure 10**a. The electroluminescence spectra (Figure 10b) of each of the derivatives featured the same S_1–S_0 transitions and excimeric peaks at higher wavelengths as the PL spectra (section 2.4). The combination of green and red electroluminescence led to an overall yellow/orange-colored emission. The CIE 193 chromaticity coordinates were: Epi, (0.60, 0.40), 2F-Epi, (0.59, 0.38), 2-Cl Epi, (0.35, 0.62). The electroluminescent performance of each material was comparable, with relatively low brightness of 10–25 cd m^{-2}. Experimenting with different growth parameters such as substrate temperature (from 30 °C up to 120 °C) and deposition rate (either slow growth of 0.1 Å s^{-1} and 5–6 Å s^{-1}) demonstrated no changes in either the brightness of the devices or the relative intensities of the singlet versus excimer emissions, again providing evidence pointing towards intrinsic excimeric species being responsible for the low-energy emission as opposed to extrinsic trap states. To evaluate the air stability of Epi OLEDs, we fabricated devices with the structure ITO/PEDOT:PSS/Epi/PEIE/Au, where PEIE = poly(ethylene imine, ethoxylated), a modification layer providing good electron-injection ability.[35] The diodes were found to emit while operating in air with a brightness of ≈15 cd m^{-2} for a period of 1 week. The low electroluminescence of these devices is a problem that may be mitigated by optimizing electron and hole injection layers to provide balanced injection of charges to increase radiative recombination in the epindolidione layer. Excimer-emitting materials are nevertheless an interesting concept to achieve polychromic emission from a single semiconducting material, and have been suggested as a possible route to achieving practical white-light emitting OLEDs.[36–38]

2.8. Solubilized Epindolidiones and Solution Processing Using the Latent Pigment Route

As described in section 2.2, epindolidiones can be functionalized with solubilizing thermolabile tBOC protecting groups. The double-substituted di-tBOC Epi shows solubility up to about 25 mg mL^{-1} in solvents like chloroform, toluene, and chlorobenzene. The mono-tBOC derivative, however, was considerably less soluble in these solvents (not higher than 1 mg mL^{-1}), though still far more soluble than unfunctionalized Epi. Uniform films of di-tBOC Epi could be obtained by spin-casting. Heating these films at 185 °C for 5 min was sufficient to achieve complete deprotection and transformation of the pale yellow di-tBOC Epi films into darker yellow films of Epi (**Figure 11**a). Absorbance and photoluminescence spectra of dilute solutions of Epi and di-tBOC-Epi are compared in Figure 11b. The optical properties of the solution-derived films, i.e., absorbance and photoluminescence, were identical to evaporated films. Unfortunately, repeated attempts to fabricate transistors using this

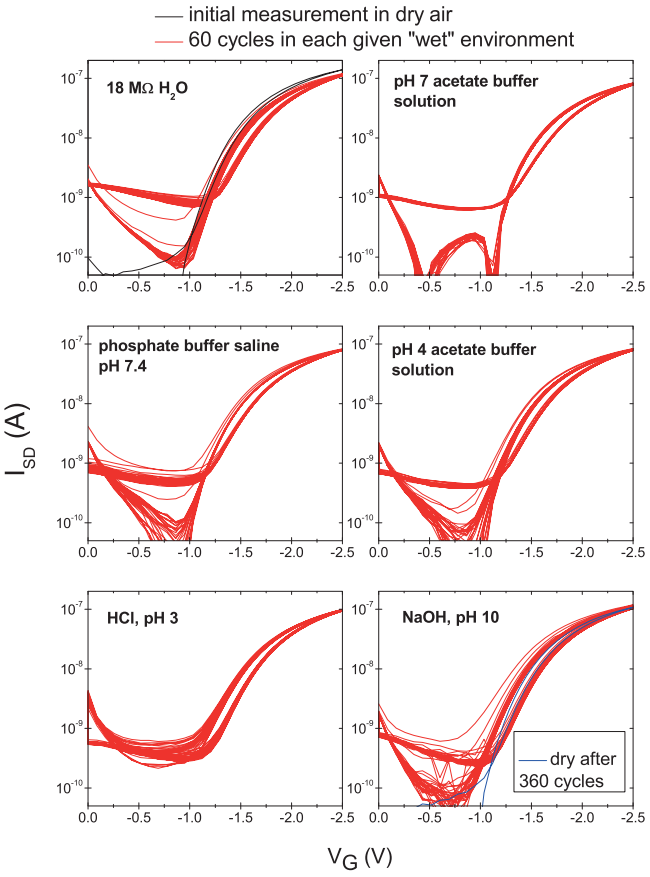

Figure 9. Low-voltage Epi transistor measured in air (black curve) and then 360 cycles in six different aqueous environments successively, with 60 cycles carried out in each. $V_{SD} = -0.5$ V. Samples were rinsed with deionized water between different electrolytes.

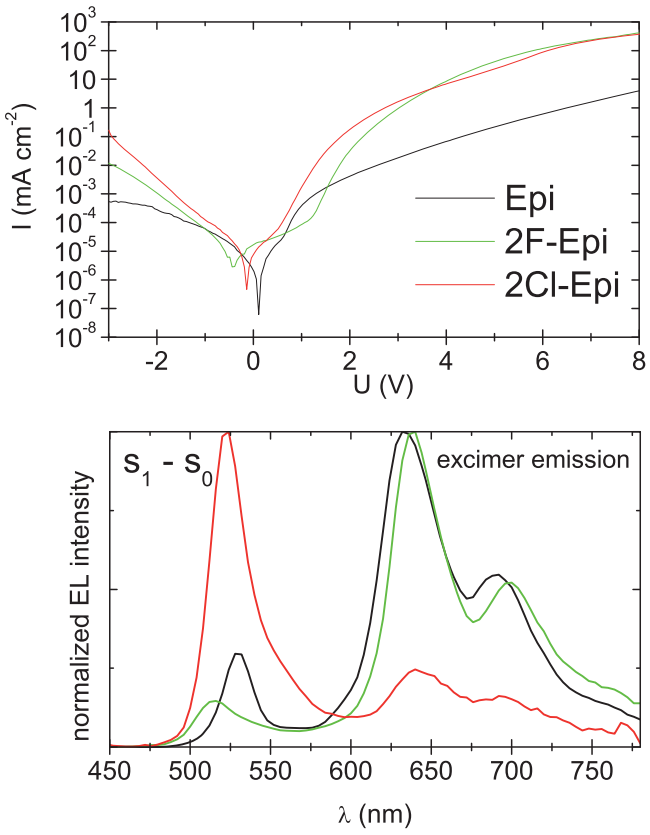

Figure 10. a) *J–V* characteristics of ITO/PEDOT:PSS/(Epi derivative)/Al diodes. b) Electroluminescence spectra of the same diodes operated in forward bias. Both the S_1-S_0 transition emitting green light and the excimers emitting yellow/red light can be observed.

method, on a variety of gate dielectric materials, yielded very poor transport. The origin of this problem is not clear, though previous studies on hydrogen-bonded pigments like indigo concluded that orientation of molecules with π–π stacking parallel to the substrate was critical, and this favorable growth is achieved via evaporation on hydrophobic substrates.[9] Diodes with the structure ITO/PEDOT:PSS/Epi/Al could be fabricated however, yielding performance indistinguishable from evaporated diodes. To obtain a pinhole-free film, a 10 mg mL^{-1} solution of di-tBOC Epi in chloroform was spin cast following heating to 185 °C for 5 min, and then a second coating followed by heating. The diodes functioned as OLEDs with the same singlet/excimer emission as the vacuum-processed devices, albeit with the same relatively low brightness values.

3. Conclusions

We have evaluated epindolidione and two halogenated derivatives in terms of their applications as organic semiconductors. Epindolidiones are a class of robust H-bonded organic pigments with a simple synthetic preparation which starts from well-known anilines. From a photophysical perspective, they are H-chromophore systems like the closely related indigos,

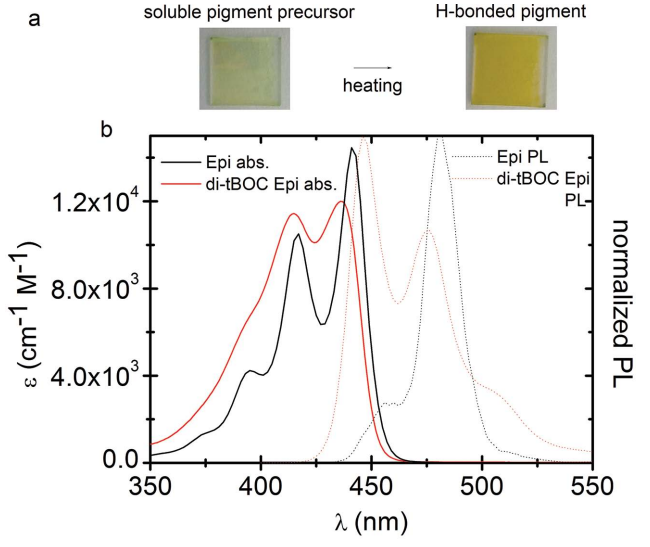

Figure 11. a) A spin-coated film on ITO-glass of di-tBOC Epi before and after thermal conversion into Epi. b) Comparison of extinction coefficients and photoluminescence of Epi and di-tBOC-Epi in dilute (≈10×10^{-6} M) chloroform solution. Epindolidione absorption shows a small, ≈4 nm, hypsochromic shift in $CHCl_3$ relative to DMSO, shown in Figure 4.

however with a hypsochromic absorption relative to indigo and a pronounced luminescence. A distinctive feature of the epindolidiones is strong excimeric emission—thus a yellow material absorbing in the blue can give strong yellow/red photoluminescence. Electrochemically, epindolidiones can be oxidized and quasi-reversibly reduced, albeit with a substantial band gap (in acetonitrile electrolyte). This translates to both electron and hole transport in transistor devices with the appropriate choice of source-drain contact metal. Low-voltage FETs fabricated with epindolidione were found to have extraordinary stability in a wide range of electrolyte solutions, wherein devices operated reliably with no degradation over hundreds of cycles. To our knowledge, no other organic semiconducting materials have demonstrated stability in such a wide range (pH 3–10 was measured here with no degradation). Due to their luminescence and ambipolarity, we found that epindolidiones can be used in electroluminescent devices, where the distinctive combination of higher-energy singlet and lower-energy excimeric electroluminescence is observed. Finally, we have presented a technique of introducing transient protecting groups (tBOC) in order to disrupt H-bonding and yield a soluble dye form of epindolidiones. This allows solution-processing techniques as well as potentially enables further chemical derivatization. This work demonstrates the potential of this highly stable pigment as a versatile organic semiconducting material. Research in industry on organic pigments has developed, over the past century, a range of highly stable heterocyclic systems synthesized from low-cost precursors. This work suggests that further insight into this class of organics as functional materials for organic electronics applications is warranted.

4. Experimental Section

Details on synthetic procedures and materials characterization data are presented in the Supporting Information. Evaporation of thin films of the Epi compounds was done using a custom-built organic evaporation system from Vaksis R&D and Engineering, allowing precise rate control and substrate heating. All thin films samples were prepared by evaporation except where otherwise noted. For UV–vis spectra, a Perkin-Elmer Lambda 950 spectrometer was used. Spectroscopic-grade DMSO was used for all optical measurements in solutions. PL spectra were recorded on a photomultiplier tube-equipped double-grating input and output fluorometer manufactured by PTI. Electrochemical measurements were carried out in a dry N_2 environment using a Pt foil as counter electrode, an Ag/AgCl wire as a pseudo-reference electrode, and ≈80 nm films of the Epi compounds vacuum evaporated on ITO as the working electrode. The supporting electrolyte was 0.1 M *n*-tetrabutylammonium hexafluorophosphate in dry acetonitrile. Frontier orbital levels were calculated according to: $E_{HOMO} = -(E_{[onset,\ ox.\ vs\ NHE]} + 4.75)$ (eV); $E_{LUMO} = -(E_{[onset,\ red.\ vs\ NHE]} + 4.75)$ (eV). Measurements were calibrated against ferrocene/ferrocenium redox couple (Fc/Fc^+). The values of the Fc/Fc^+ versus NHE and NHE versus vacuum level used in this work were 0.64 and –4.75 V, respectively.[39] ITO glass slides used for electrochemistry and diode fabrication were cleaned sequentially with acetone, isopropanol, detergent, and DI water, and finally treated with O_2 plasma. Glass slides for OFET fabrication were prepared in the same way. Aluminum/aluminum Oxide/TTC gate structures were prepared according to reported methods.[40,41] 80 nm films of the Epi compounds were vacuum evaporated at a rate of 0.5Å s^{-1}. For low-voltage OFETs optimized for operation in aqueous environments, ultrathin aluminum oxide layers (≈8 nm) were prepared using the potentiostatic method[33,42] with a 5 V anodization voltage, treated for 1 min in oxygen plasma to active the surface, and passivated with n-octadeceylphosphonic acid (C18-PA) according to reported methods,[43] by immersing for 12 h in a C18-PA 5 mM solution in isopropanol. The samples were rinsed with isopropanol and water and then heated in vacuo at 110 °C prior to evaporation of the epindolidione semiconductor layer. OFET properties were measured using an Agilent B1500A parameter analyzer in ambient air environment. The quantitative electroluminescence spectra was measured using a Photo Research Spectrascan PR-655. IV measurements were carried out with a Keithley 2600 source measurement unit.

Supporting Information

Supporting Information is available from the Wiley Online Library or from the author.

Acknowledgements

The authors are grateful for support by the Austrian Science Foundation, FWF, within the Wittgenstein Prize of N. S. Sariciftci Solare Energie Umwandlung Z222-N19 and the Translational Research Project TRP 294-N19 "Indigo: From ancient dye to modern high-performance organic electronics circuits." Italian MIUR – PON project "Molecular Nanotechnologies for Health and Environment-MAAT" (PON02_005633316357 – CUP B31C12001230005) is also acknowledged.

Received: July 29, 2014
Revised: November 13, 2014
Published online: December 22, 2014

[1] H. Zollinger, *Color Chemistry. Syntheses, Properties and Applications of Organic Dyes and Pigments* 3rd ed.; Wiley-VCH, Weinheim **2003**.
[2] *High Performance Pigments* (Eds: E. B. Faulkner, R. J. Schwartz) 2nd ed., Wiley-VCH, Weinheim **2009**.
[3] M. Seefelder, *Indigo in culture, science, and technology*, 2nd ed., ecomed: Landsberg, Germany **1994**.
[4] K. Hunger, *Rev. Prog. Color. Relat. Top.* **2005**, *35*, 76.
[5] G. De Luca, W. Pisula, D. Credgington, E. Treossi, O. Fenwick, G. M. Lazzerini, R. Dabirian, E. Orgiu, A. Liscio, V. Palermo, K. Müllen, F. Cacialli, P. Samorì, *Adv. Funct. Mater.* **2011**, *21*, 1279.
[6] D. Görl, X. Zhang, F. Würthner, *Angew. Chem. Int. Ed.* **2012**, *51*, 6328.
[7] M. Irimia-Vladu, E. D. Głowacki, P. A. Troshin, G. Schwabegger, L. Leonat, D. K. Susarova, O. Krystal, M. Ullah, Y. Kanbur, M. A. Bodea, V. F. Razumov, H. Sitter, S. Bauer, N. S. Sariciftci, *Adv. Mater.* **2012**, *24*, 375.
[8] E. D. Głowacki, L. Leonat, G. Voss, M.-A. Bodea, Z. Bozkurt, A. M. Ramil, M. Irimia-Vladu, S. Bauer, N. S. Sariciftci, *AIP Adv.* **2011**, *1*, 042132.
[9] E. D. Głowacki, G. Voss, N. S. Sariciftci, *Adv. Mater.* **2013**, *25*, 6783.
[10] E. D. Głowacki, M. Irimia-Vladu, M. Kaltenbrunner, J. Gąsiorowski, M. S. White, U. Monkowius, G. Romanazzi, G. P. Suranna, P. Mastrorilli, T. Sekitani, S. Bauer, T. Someya, L. Torsi, N. S. Sariciftci, *Adv. Mater.* **2013**, *25*, 1563.
[11] E. D. Głowacki, L. Leonat, M. Irimia-Vladu, R. Schwo diauer, M. Ullah, H. Sitter, S. Bauer, N. Serdar Sariciftci, *Appl. Phys. Lett.* **2012**, *101*, 023305.
[12] W. Herbst, K. Hunger, *Industrial Organic Pigments*, 3rd ed., Wiley-VCH: Weinheim, **2004**.
[13] S. Yamazaki, L. Sobolewski, W. Domcke, *Phys. Chem. Chem. Phys.* **2011**, *13*, 1618.
[14] E. E. Jaffe, *J. Oil Colour Chem. Assoc.* **1992**, *75*, 24.

[15] D. S. Kemp, B. R. Bowen, C. C. Muendel, *J. Org. Chem.* **1990**, *55*, 4650.
[16] U. Schaedeli, J. S. Zambounis, A. Iqbal, Z. Hao, H. Dubas, *EP 0654711* **1993**.
[17] J. S. Zambounis, Z. Hao, A. Iqbal, *Nature* **1997**, *388*, 131.
[18] E. D. Glowacki, G. Voss, K. Demirak, M. Havlicek, N. Sunger, A. C. Okur, U. Monkowius, J. Gasiorowski, L. Leonat, N. S. Sariciftci, *Chem. Commun.* **2013**.*49,* 6063.
[19] G. Lincke, *Dyes Pigm.* **2000**, *44*, 101.
[20] G. Lincke, *Dyes Pigm.* **2002**, *52*, 169.
[21] E. F. Paulus, F. J. J. Leusen, M. U. Schmidt, *CrystEngComm* **2007**, *9*, 131.
[22] E. D. Głowacki, H. Coskun, M. a. Blood-Forsythe, U. Monkowius, L. Leonat, M. Grzybowski, D. Gryko, M. S. White, A. Aspuru-Guzik, N. S. Sariciftci, *Org. Electron.* **2014**, *15*, 3521.
[23] L. Grehn, U. Ragnarsson, *Angew. Chem. Int. Ed.* **1984**, *23*, 296.
[24] W. Lüttke, H. Hermann, M. Klessinger, *Angew. Chem. Int. Ed.* **1966**, *5*, 598.
[25] W. Tuer, Epindolidione, Epindoline und lineare sowie trigonale Imidazolderivate - Neue Materialien mit interessanten Fluoreszenzeigenschaften, PhD dissertation, Ludwig-Maximilians-University Munich, 2001.
[26] H. Sieghold, Synthesen und Spektroskopisches Verhalten von Heteroanalogen Carbonylindigo-farbstoffen, PhD dissertation, University of Göttingen, 1973.
[27] A. Amat, F. Rosi, C. Miliani, A. Sgamellotti, S. Fantacci, *J. Mol. Struct.* **2011**, *993*, 43.
[28] J. Mizuguchi, *Ber. Bunsengesellsch. Phys. Chem.* **1993**, *97*, 684.
[29] L. Rossi, G. Bongiovanni, J. Kalinowski, G. Lanzani, A. Mura, M. Nisoli, R. Tubino, *Chem. Phys. Lett.* **1996**, *257*, 545.
[30] L. Rossi, G. Bongiovanni, A Borghesi, G. Lanzani, J. Kalinowski, A. Mura, R. Tubino, *Synth. Met.* **1997**, *84*, 873.
[31] D. Braga, G. Horowitz, *Adv. Mater.* **2009**, *21*, 1473.
[32] L. Torsi, M. Magliulo, K. Manoli, G. Palazzo, *Chem. Soc. Rev.* **2013**, *42*, 8612.
[33] A. I. Mardare, M. Kaltenbrunner, N. S. Sariciftci, S. Bauer, A. W. Hassel, *Phys. Status Solidi A* **2012**, *209*, 813.
[34] M. E. Roberts, S. C. B. Mannsfeld, N. Queraltó, C. Reese, J. Locklin, W. Knoll, Z. Bao, *Proc. Natl. Acad. Sci. U.S.A.* **2008**, *105*, 12134.
[35] Y. Zhou, C. Fuentes-Hernandez, J. Shim, J. Meyer, A. J. Giordano, H. Li, P. Winget, T. Papadopoulos, H. Cheun, J. Kim, M. Fenoll, A. Dindar, W. Haske, E. Najafabadi, T. M. Khan, H. Sojoudi, S. Barlow, S. Graham, J.-L. Bredas, S. R. Marder, A. Kahn, B. Kippelen, *Science* **2012**, *336*, 327.
[36] J. Kalinowski, G. Giro, M. Cocchi, V. Fattori, P. Di Marco, *Appl. Phys. Lett.* **2000**, *76*, 2352.
[37] G. M. Farinola, R. Ragni, *Chem. Soc. Rev.* **2011**, *40*, 3467.
[38] X. Yang, Z. Wang, S. Madakuni, J. Li, G. E. Jabbour, *Adv. Mater.* **2008**, *20*, 2405.
[39] C. M. Cardona, W. Li, A. E. Kaifer, D. Stockdale, G. C. Bazan, *Adv. Mater.* **2011**, *23*, 2367.
[40] M. Kraus, S. Richler, A. Opitz, W. Brütting, S. Haas, T. Hasegawa, A. Hinderhofer, F. Schreiber, *J. Appl. Phys.* **2010**, *107*, 094503.
[41] E. D. Głowacki, M. Irimia-Vladu, S. Bauer, N. S. Sariciftci, *J. Mater. Chem. B* **2013**, *1*, 3742.
[42] M. M. Lohrengel, *Mater. Sci. Eng. R* **1993**, *11*, 243.
[43] M. Kaltenbrunner, T. Sekitani, J. Reeder, T. Yokota, K. Kuribara, T. Tokuhara, M. Drack, R. Schwödiauer, I. Graz, S. Bauer-Gogonea, S. Bauer, T. Someya, *Nature* **2013**, *499*, 458.